Microfabrication of single-crystal silicon multiple torsional oscillators

Michelle D. Chabot and John T. Markert

Department of Physics
University of Texas at Austin
Austin, Texas 78712

ABSTRACT

Micro-oscillators of different designs and dimensions have been fabricated for use in a nuclear magnetic resonance force microscope. The various designs include double and triple torsional oscillators which have high Q's at room temperature ($\approx 10,000$) when operating at the upper cantilever and upper torsional resonances. Depending on design and dimensions, the resonance frequencies vary from tens to hundreds of kHz. Typical dimensions of the designs are (200×150) μm^2 $\times$ 200 nm thick. To fabricate these devices, microelectronic fabrication techniques were employed. Si (100) wafers were patterned, etched, and boron-implanted at a dose of 4.2×10^{16} cm^{-2} and an energy of 134 keV. A post-implant anneal was then performed at 1000°C, followed by a KOH wet-etch which leaves the free-standing boron-doped oscillators. Depending on the doping level, anneal, and etch parameters, the thickness of the oscillators varies from 100–400 nm. In order to optimize the design and fabrication process, resonance frequencies and Q's have been characterized using fiber-optic interferometry. For example, the upper cantilever resonance of one design has been found to have a minimum detectable force of 1.5 x 10^{-16} N/$\sqrt{\text{Hz}}$ at room temperature.

Keywords: Micro-oscillators, MRFM, high-Q

1. INTRODUCTION

Micro-oscillators of various designs have become useful tools in many applications which require good sensitivity. In particular, applications which measure small forces benefit from low damping and low spring constant. These two requirements have been achieved by creating single-crystal silicon multiple torsional oscillators using microelectronic fabrication techniques. This process will be detailed, and results of the oscillator characterization will be given which demonstrate their minimum detectable force capabilities.

2. DESIGN MOTIVATION

2.1. Nuclear Magnetic Resonance Force Microscopy

Nuclear Magnetic Resonance Force Microscopy (NMRFM) is a novel technique for detecting an NMR signal through direct force measurement.[1–4] This application has been the motivation for the creation of these micro-oscillators. A brief background is necessary to understand the considerations which went into the torsional design.

In conventional NMR, the precessing magnetization is detected through an induced voltage in a pick-up coil. Our NMRFM instead couples the magnetization to to a mechanical oscillator and then uses fiber optic interferometry to detect the motion. A small magnet is used to create a strong field gradient in the region of the sample which is to be scanned. An rf field is applied which causes the nuclear moments in the sample to oscillate at the resonance frequency of the mechanical oscillator. This oscillating magnetization in the field gradient results in an oscillating force, also at the resonance frequency of the mechanical oscillator. The motion is detected through fiber optic interferometry, and the amplitude of oscillation determines the force on the oscillator due to the moments in a resonance slice of the sample.

Send correspondence to J. T. Markert; E-mail: markert@physics.utexas.edu

The force sensitivity achievable through this process is ultimately limited by the thermal noise of the mechanical oscillator, given in $N/\sqrt{Hz}$ by

$$F_{min} = \sqrt{\frac{4k_BTk}{Q\omega}}, \tag{1}$$

where Q is the quality factor, k is the spring constant, T is the temperature, and ω is the resonant frequency of the oscillator. Therefore, a high Q (low damping) and a low spring constant will decrease the minimum detectable force. It has been theorized that with a strong enough field gradient to create a small enough resonance slice single spin detection is possible with NMRFM.[5] Thus this is a feasible method for scanning a sample in three dimensions with atomic resolution. However, many improvements are needed to achieve this goal.

To further the effort to increase the sensitivity, oscillators need to be fabricated which have a low enough thermal noise, yet which still have a sturdy enough design to be feasible for use in an NMRFM.

2.2. Multiple Torsional Design

Fig. 1 shows the two main designs which are used to achieve the lowest damping. Larger double-torsional oscillators have already been successfully used to detect small forces in superconductors.[6] The double-torsional oscillator[7] in Fig. 1(a) has fours main resonances: the upper and lower cantilever modes and the upper and lower torsional modes. In the upper torsional and cantilever modes the 'head' moves opposite the 'wing'. Since single crystal silicon is used to minimize losses dye to defects, most dissipation occurs through coupling to the base. The upper resonances will have less damping since the energy of oscillation is mainly contained in the 'head', which is relatively isolated from the base. For the upper torsional mode, the stored energies are related by[8]

$$E_{head} = \frac{I_{wing}}{I_{head}} E_{wing}, \tag{2}$$

where I is the moment inertia. Since $I_{wing}/I_{head} \gg 1$, $E_{head} \gg E_{wing}$. Therefore, the stored energy is isolated in the head, and a high Q will be achieved.

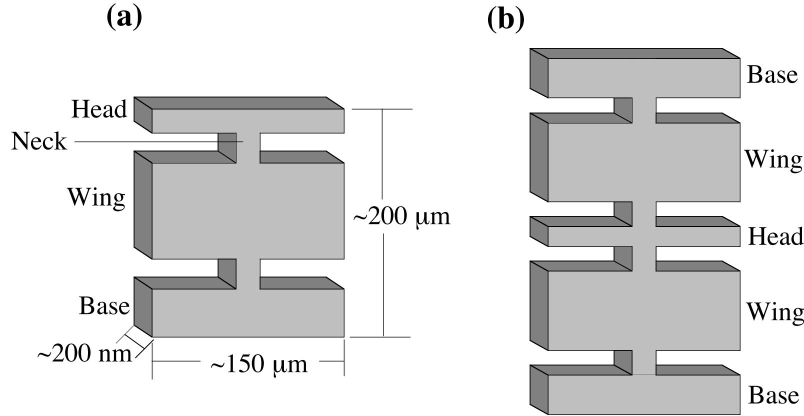

Figure 1. (a) Double-torsional design. (b) Triple-torsional design.

The other main consideration in the design was the desire to have a low spring constant. The spring constant for the torsional modes can be estimated by:[9,10]

$$\kappa \approx \frac{Gwt^3}{h}\left[\frac{1}{3} - 0.209\frac{t}{w}\left(1 - \frac{1}{12}\left(\frac{t}{w}\right)^4\right)\right], \tag{3}$$

where G is the shear modulus, t is the thickness of the oscillator, and w and h are the width and the height, respectively, of the neck. From this, it is clear that the spring constant will be decreased by decreasing the size (and therefore the thickness) of the oscillators. However, the size and thickness can not be decreased too much due to practical limitations of NMRFM. Samples (or magnets) need to be mounted onto the oscillators, so they must be large enough so that their resonances will not be greatly affected by the extra weight. Also, they must be sturdy enough to withstand the mounting process. Therefore, the designs in Fig. 1 have been made to be an average size of 200 μm tall, 150 μm wide, and 200 nm thick.

Triple torsional designs (Fig. 1(b)) have also been fabricated to increase the sturdiness of the oscillators. The etching process which will be described in Section 3 can cause the oscillators to bend slightly. The triple torsional design, since it is connected at both ends, avoids this problem while still maintaining a high Q and low spring constant.

The resonant frequencies of each design were calculated before processing efforts began. This was done by estimating the form of the spring constant and assuming a classical harmonic system. For example, the torsional resonances are estimated by solving the ideal equations of motion for the 'head' and the 'wing':

$$\begin{aligned} I_h \theta_h + k\left(\theta_h - \theta_w\right) &= 0 \\ I_w \theta_w + k\theta_w - k\left(\theta_h - \theta_w\right) &= 0, \end{aligned} \tag{4}$$

where $\theta_i = A_i e^{-i\omega t}$. The spring constant is known from (3), and the moments of inertia can be calculated from the dimensions of the oscillators and the density of silicon. Therefore the normal mode frequencies can be solved for numerically. This was done, and the dimensions of the designs were chosen so that the frequency of the upper torsional mode fell between 50 and 100 kHz. This process was also done before designing the mask for the triple torsional designs. Again, the dimensions were chosen to keep the largest normal mode frequency under 100 kHz.

3. FABRICATION PROCESS

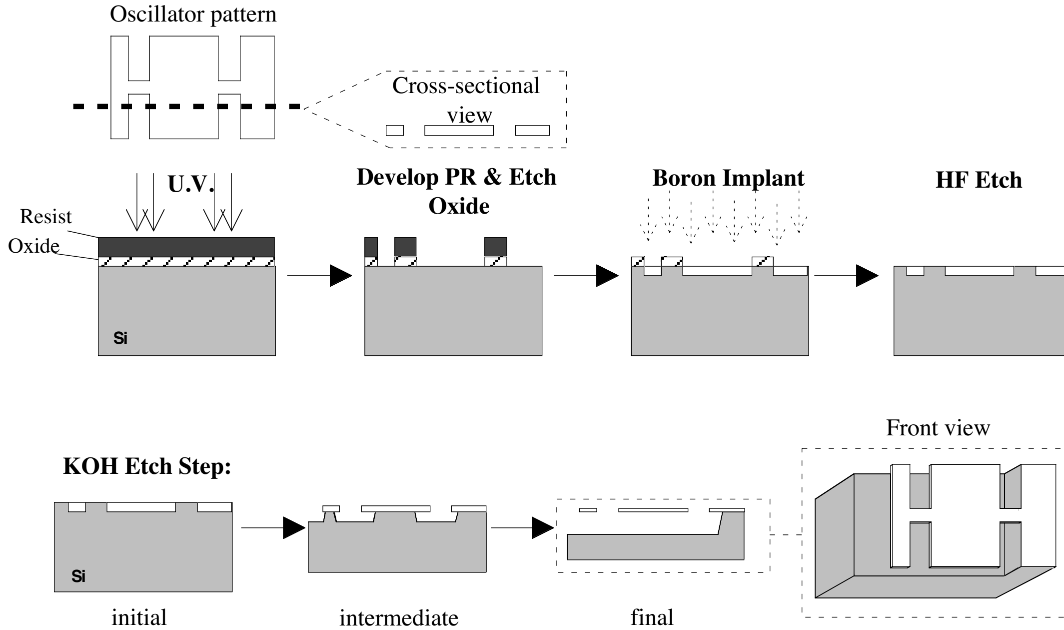

Figure 2. Process outline for the fabrication of multi-torsional oscillators.

The oscillators were fabricated by following the process outlined in Fig. 2. Single crystal silicon (100) wafers with 7500 $\mathring{A}$ of oxide pre-grown on them were used. Currently, the process requires only one photolithography step, so no multiple alignment patterns are necessary.

3.1. Wafer Patterning

The first step in the processing is the generation of a mask with the desired pattern. An example of one such mask is given in Fig. 3. The pattern is first drawn on a computer with 100 times magnification to avoid limitations due to poor printer quality. Then the pattern is photo-reduced to its final 1 cm^2 size. The negative is then used to expose the mask using a positive photoresist. The pattern is exposed approximately 40 times onto one mask so that each 4" (100) wafer will result in 40 individual chips, each containing approximately 150 oscillators. Once the mask is exposed, it is developed, post-baked, and the iron oxide is etched away.

The mask is then used to expose the silicon wafer with a positive photoresist on it. The mask is aligned so that the base of the oscillators is parallel to the wafer flat. This is to allow for the best etching planes. The exposed wafers are then developed and the oxide is etched away using a reactive ion etch with an oxygen and freon plasma.

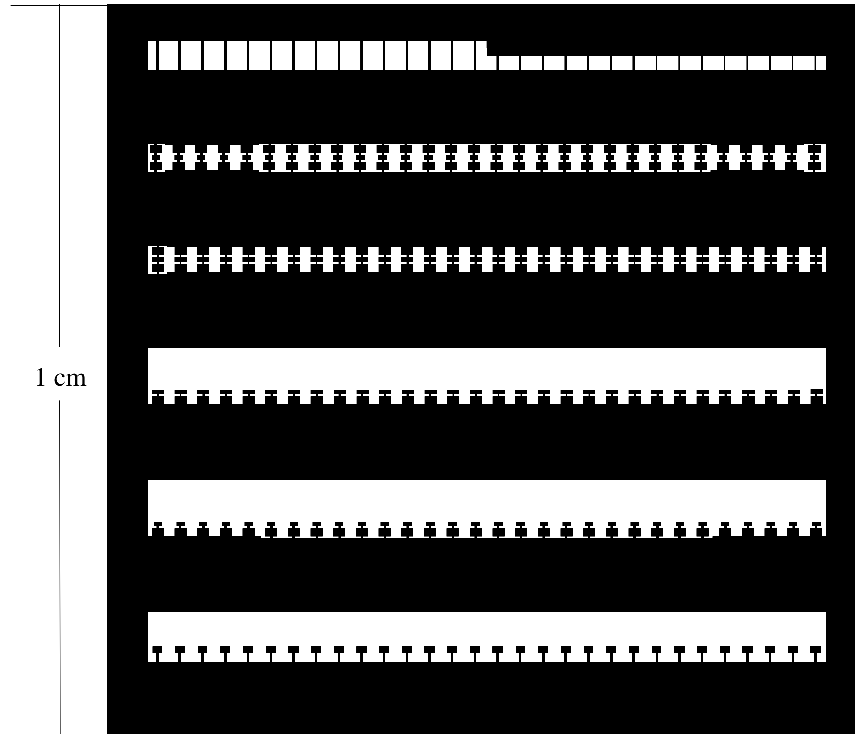

Figure 3. One mask pattern used to fabricate the multi-torsional oscillators.

3.2. Boron Implant

Once the oxide has been etched, the exposed areas of the wafer correspond to the location of the oscillators. Boron is implanted into these exposed regions at an energy of 134 keV and a dose on the order of 10^{16} ions/cm^2. The energy was chosen because it yields a peak implant of 400 nm. The initial 7500 $\mathring{A}$ thick oxide was chosen because this is the thickness needed to stop more than 99.99% of the boron for this energy.[11] The dose has been varied from 1.4 x 10^{16} ions/cm^2 to 4.2 x 10^{16} ions/cm^2.

After implanting, an anneal at 1000°C is performed to repair implant damage. This step broadens the steep Gaussian profile and therefore is a main factor in the final thickness of the oscillators. However, this broadening needs to be kept small so that the boron concentration in the area of the oscillators is kept large enough ($> 7 \times 10^{19}$ cm^{-2}) to stop the KOH wet-etch descibed in the next section. Therefore, the higher dose with a short anneal time (1/2 – 3 hr) has produced the best oscillators, with thicknesses in the original 100 – 400 nm target range.

After the implant, the 4" wafer is sliced so that 40 individual chips are obtained. A buffered HF etch is done to remove the remaining oxide from each chip. The 1 cm^2 chip is now ready for the KOH etch.

3.3. Final Etch

The most critical processing step is the final wet-etch. This step is an anisotropic, differential etch using potassium hydroxide (KOH) mixed with water and ethanol. The heavily boron-doped silicon serves as an etch-stop, since the etch rate of p++ silicon in KOH is much lower than that of undoped silicon.[12,13] Varying the concentrations in the etch solution had a small effect on the quality of the oscillators after the etch, and it was determined that the optimal mixture consists of 125 g KOH, 300 ml distilled water, and 200 ml of ethanol. The temperature dependence on the etch was also investigated, and this was found to have a much greater effect. It was determined that decreasing the temperature provided much better differential etching. Thus, the best oscillators were found using an etch near 0°C (in an ice bath).

These optimal etch parameters result in several days of slow etching. For non-differential etching of pure silicon, it is common to etch at 80○C, giving an etch rate of approximately 1 μm/min[13]. However, Fig. 2 illustrates the reason a very good differential etch is necessary. When etching from the front, the etchant must eat around the oscillators and behind them. There is an absolute minima in the etch rate for $\langle 111 \rangle$ directions, and relative minima for $\langle 110 \rangle$ directions.[14] The etch is partly done in these slow etch directions, resulting in a relatively long etch time. Typically about 100 μm of silicon are etched while preserving the 0.4 μm thick oscillators. For many regions of parameter space, the oscillators were completely etched away during this process.

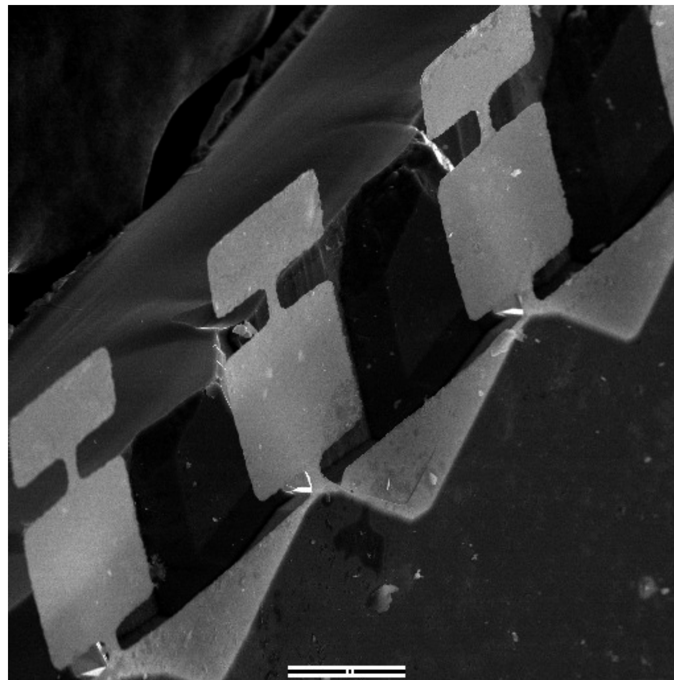

Figure 4. A typical row of double-torsional oscillators.

3.4. Extraction: Overcoming Stiction

When the oscillators come out of the etch, surface tension brings them in contact with the silicon back and various forces, such as van der Waals forces, keep them stuck even after they have dried completely.[15,16] An accessible method for overcoming this problem involves rinsing the still-submerged oscillators in a solution of water and ethanol. The wet chip is then frozen by applying a vacuum and continuously pumped on until the frozen solution sublimates. Thus there is no surface tension which makes the oscillators contact the silicon below, and stiction is avoided.

Fig. 4 shows a typical row of completed double-torsional oscillators. SEM images indicate that oscillators have been successfully made with thicknesses ranging from 100 to 400 nm. These correspond to the various doses used during the implant process step.

4. CHARACTERIZATION APPARATUS

Once the oscillators had been successfully etched, they were characterized to determine the Q, frequency, and approximate spring constant, thereby determining the minimum detectable force capabilities. This was done using the components of the NMRFM described in Section 2. Fig. 5 gives an overview of the testing set-up. The oscillator is mounted on a piezo shaker linked to a computer-controlled frequency generator. A feedback circuit,

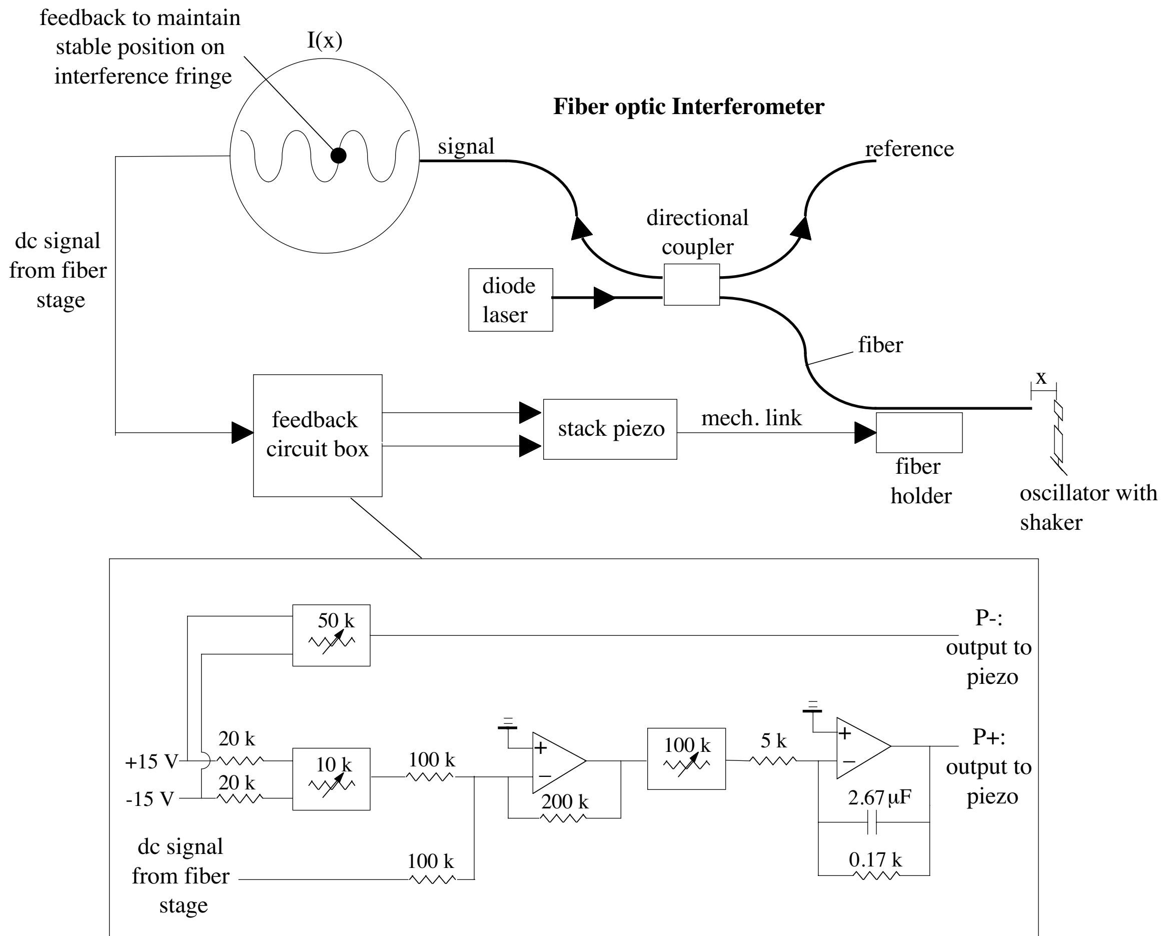

Figure 5. Overview of apparatus used for the characterization of the oscillators.

shown at the bottom of Fig. 5, maintains the optical fiber on a stable fringe and allows for fine positioning perpendicular to the oscillator. The interference signal is sent to a lock-in amplifier. Frequency scans are done, and the oscillation amplitude and phase are recorded for analysis. The detection limitation of this apparatus is less than 0.001 nm/$\sqrt{\text{Hz}}$.

5. RESONANCE RESULTS

The dimensions and spring constants of the oscillators are known within reasonable uncertainty limits from design, measurements, and modeling. Measurement of the resonant frequencies and quality factors therefore determines their force sensitivity.

5.1. Observed Resonances

Figure 6 shows a typical frequency sweep of one micro-oscillator. Four resonances are generally evident. These are assigned, in order of increasing frequency, to the lower cantilever, lower torsional, upper cantilever, and upper torsional modes. The type of mode has been verified by moving the interferometer laser spot to various points on the oscillator while maintaining the same excitation signal. For the lower (symmetric) cantilever mode, both sides of the head and both sides of the wing move in phase. For the lower torsional, both sides of the head and both sides of the wing move with opposite phase, and the same side on the head and wing move together. Similiar tests have verified the upper (antisymmetric) resonance modes as well.

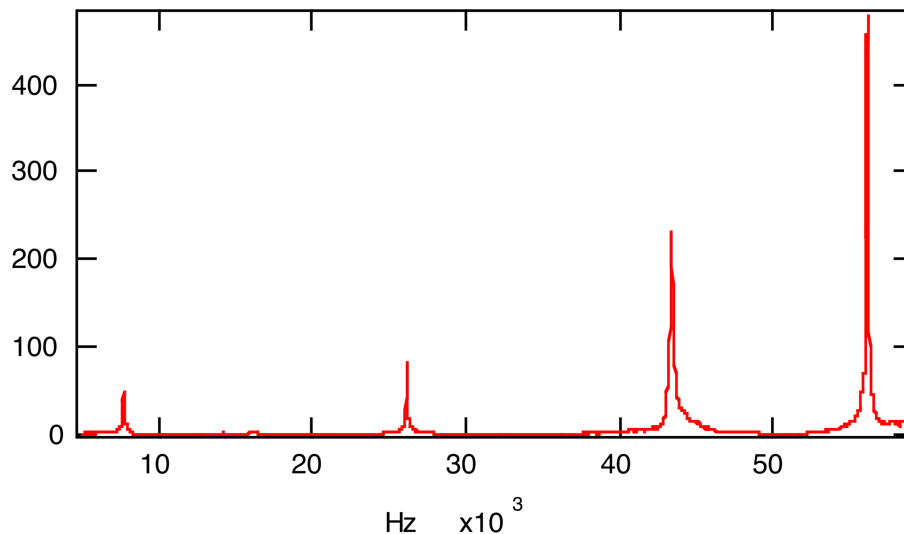

Figure 6. Typical frequency scan obtained for one micro-oscillator, demonstrating the four main resonances.

The location of the resonance frequencies did not change greatly for the different dimensions in the double-torsional designs. Table 1 shows the range in which the four resonances fell for oscillator of nominal thickness 400 nm scanned at room temperature.

When designing the triple-torsional oscillators, the dimensions were chosen so that the predicted value for the upper torsional mode (head moves opposite to both wings) fell between 50 and 90 kHz for 400 nm thickness. Since the double-torsional resonances fell in the calculated range (determined by assuming a simple classical harmonic system), it is expected that the triple-torsional resonances will also lie below 100 kHz. Since the triple-oscillator was designed to be symmetric about the head, there are three torsional resonances of the design, labeled the lower, middle, and upper modes. The upper mode will once again be the one of interest since it offers the least coupling to the bases and therefore the lowest damping. It is also possible to observe 'guitar-string' resonances for the designs which are mounted on both ends. To be able to examine this possibility, simple bars attached

Table 1. Resonant frequency ranges for the double-torsional oscillators with thicknesses ≈ 400 nm.

Mode	Frequency Range
Lower cantilever	5 - 15 kHz
Lower torsional	25 - 35 kHz
Upper cantilever	35 - 50 kHz
Upper torsional	50 - 70 kHz

at both ends were designed, as shown in the top row in the mask in Figure 3. Because the double-torsional oscillators have the easily-observed cantilever resonances, these are the ones used for the characterization results.

The sharpness of the resonance peaks in Fig. 6 demonstrates the high-Q capabilities of the oscillators. This feature is highlighted in Fig. 7, which shows a comparison of a commercial AFM cantilever resonance to one of the higher-Q micro-oscillator resonances obtained at room temperature. Whereas the amorphous commercial oscillator has a low Q ≈ 10, the single crystal double oscillator has a Q $\approx 10,000$. This value is expected to increase when the system is cooled.

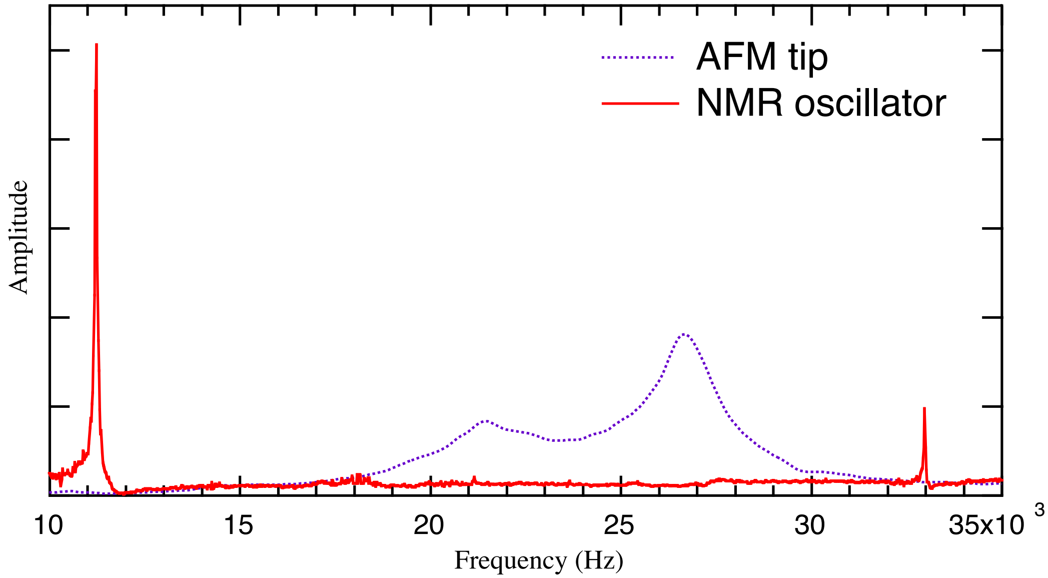

Figure 7. Comparison of double-torsional oscillator resonance to commercial AFM cantilever.

5.2. Sensitivity Evaluation

The Q's for the upper resonances of the oscillators (regardless of the different lateral dimensions) are generally on the order of 10,000 at room temperature. Using this value, along with a typical value of the effective spring constant $k \approx 5 \times 10^{-3}$ N/m (for a 300 nm thick oscillator), the force sensitivity is (for a 62 kHz mode):

$$F_{min} = 1.5 \times 10^{-16} \mathrm{N}/\sqrt{\mathrm{Hz}} \quad (5)$$

This value demonstrates the advantage of using the multi-torsional oscillator design. Much higher sensitivity is expected for lower temperature and thinner oscillators.

6. CONCLUSIONS

Multi-torsional oscillators have been designed, fabricated, and the resonances observed. They have been designed with the particular application of the NMR force microscope in mind, and therefore have been made small but sturdy, with low spring constants and high Q's. Although they were initially fabricated for this purpose, the good results achieved thus far indicate that they are also feasible for commercial use. This effort is currently underway. The KOH wet-etch step has been shown to be the most critical process step, and it was found that the best differential etch is achieved at low temperatures. The typical resulting oscillator thickness, depending on the implant and anneal, ranges from 100 – 400 nm. It has been shown that, even for non-optimal conditions, the force sensitivity of these oscillators is a large improvement over commercial cantilevers, with a value at room temperature of $F_{min} = 1.5 \text{ x } 10^{-16}\text{N}/\sqrt{\text{Hz}}$. At helium temperature, the Q typically increases by 1000 (determined from experiments made on larger torsional oscillators). This improvement, along with design improvements to further decrease the spring constant, yields a projected value for the force sensitivity at 1.5 K: $F_{min} = 1.5 \times 10^{-19}$ $\text{N}/\sqrt{\text{Hz}}$. Thus the multiple torsional design will be a large factor in achieving the desired sensitivity for atomic scale NMRFM.

ACKNOWLEDGMENTS

This work was supported by the U.S. Army Grant No. DAA G55-98-C-0070, the National Science Foundation Grant No. DMR-9705414, and the Robert A. Welch Foundation Grant No. F-1191.

REFERENCES

1.D. Rugar, C. S. Yannoni, and J. A. Sidles, "Mechanical detection of magnetic resonance," *Nature* **360**, pp. 563-566, 1992.

2. D. Rugar, O. Zuger, S. Hoen, C. S. Yannoni, H. M. Vieth, and R. D. Kendrick, "Force detection of nuclear magnetic resonance," *Science* **264**, pp. 1560-1563, 1994.

3. O. Zuger and D. Rugar, "Magnetic resonsnce detection and imaging using force microscope techniques (invited)," *J. Appl. Phys.* **75**, pp. 6211-6216, 1994.

4. T. A. Barrett, C. R. Miers, H. A. Sommer, K. Mochizuki, and J. T. Markert, "Design and construction of a sensitive nuclear magnetic resonance force microscope," *J. Appl. Phys.* **8**3, pp. 6235-6237, 1998.

5. J. A. Sidles, J. L. Garbini, and G. P. Drobny, "The theory of oscillator-coupled magnetic resonance with potential applications to molecular imaging," *Rev. Sci. Instrum.* **63**, pp. 3881-3899, 1992.

6. A. L. Barr and J. T. Markert, "Fine structure in a high-resolution vortex dissipation study of $\text{YBa}_2\text{Cu}_3\text{O}_{7-\delta}$," *Phys. Rev. Lett.* **77**, pp. 731-734, 1996.

7. R. N. Kleimanm, G. K. Kaminsky, J. D. Reppy, R. Pindak, and D. J. Bishop, "Single-crystal silicon high-Q torsional oscillators," *Rev. Sci. Instrum.* **56**, pp. 2088-2091, 1985.

8. A. L. Barr, *Dissipation Studies of* $Y_1Ba_2Cu_3O_7$ *Using Torsional Oscillators*, Dissertation: University of Texas at Austin, 1996.

9. S. D. Timoshenko and J. N. Goodier, *Theory of Elasticity*, McGraw-Hill, New York, 1970.

10. W. C. Young, *Roark's Formulas for Stress and Strain*, McGraw-Hill, New York, 1989.

11. S. K. Ghandi, *VLSI Fabrication Principles*, chap. 6, John Wiley and Sons, New York, 1983.

12. E. D. Palik, J. W. Faust, Jr., H. F. Gray, and P. F. Green, "Study of the etch-stop mechanism in silicon," *J. Electrocham. Soc.* **129**, pp. 2051-2058, 1982.

13. S. K. Ghandi, *VLSI Fabrication Principles*, chap. 9, John Wiley and Sons, New York, 1983.

14. M. Elwenspoek, "The form of etch rate minima in wet chemical anisotropic etching of silicon," *J. Micromech. Microeng.* **6**, pp. 405-409, 1996.

15. R. Legtenberg, "Stiction of surface micromachined structures after rinsing and drying: model and investigation of adhesion mechanisms," *Sensors and Actuators A* **43**, pp. 230-238, 1994.

16. P. Scheeper, J. Voorthuyzen, W. Olthuis, and P. Bergveld, "Investigation of attractive forces between PECVD silicon nitride microstructures and an oxidized silicon substrate," *Sensors and Actuators A* **30**, pp. 230-238, 1992.